Quantum Electronics **51** (10) 894–900 (2021)

https://doi.org/10.1070/QEL17610

Triple-clad optical fibre for pulse stretching

K.K. Bobkov, A.E. Levchenko, M.Yu. Salganskii,
D.V. Ganin, A.D. Lyashedko, D.V. Khudyakov, M.E. Likhachev

Abstract. **This paper presents triple-clad stretcher fibre designs in which second-, third-, and fourth-order dispersion is matched to that of a grating-pair compressor in the Treacy configuration. The use of fibre having one of the proposed designs in a chirped pulse amplifier has made it possible to produce an all-fibre very large pulse stretching system that allows one to ensure the best possible quality of stretched pulse compression to a femtosecond duration.**

Keywords: *triple-clad optical fibre, pulse stretching, chirped pulse amplifier.*

1. Introduction

Fibre sources of femtosecond pulses with a centre wavelength in the 1 μm range and a high peak power have attracted great interest owing to the diversity of their practical applications (in particular in industry and medicine for precision processing of materials having low thermal stability). It is fibre lasers that are used for this purpose because they are compact and relatively cheap, without components requiring adjustment. Since optical fibre is per se a medium with a rather low threshold for nonlinear effects, to achieve a high peak power of fibre lasers it is necessary to use a large mode area (LMA) active fibre and a so-called chirped pulse amplifier (CPA) scheme. Its principle is that pulses from a master oscillator (as a rule, a few hundred femtoseconds in duration) are first stretched by a factor of 100 to 1000, then amplified in an LMA active fibre, and compressed to their original duration in an ideal case. Silica glass, a basic material of optical fibre for operation in the 1 μm range, has a normal second-order dispersion ($\beta_2 > 0$). Therefore, a compressor with an anomalous second-order dispersion should be used for pulse compression. However, at large pulse stretching–compression ratios, not only second-order dispersion but also at least third-order one should be compensated to achieve the best compressed pulse quality (pedestal-free pulses of the minimum possible duration). In standard silica fibre and grating compressors, third-order dispersion has the same sign ($\beta_3 > 0$). To control the sign of the third-order dispersion, it was proposed previously that W profile fibre (see e.g. Ref. [1]) or triple-clad fibre [2, 3] should be used, but the capabilities of these approaches were not examined in detail.

In this work, numerical simulation is used to optimise the triple-clad fibre design in order to match the fibre to grating compressor dispersion and assess the feasibility of its practical implementation. We demonstrate that, by optimising fibre parameters and then the compressor design (tuning the grating angle and simultaneously matching the grating separation and fibre length), it is possible to obtain compensable dispersion in a broad spectral range (more than 20 nm in the case of pulse compression to a duration less than 1 ps). Using the proposed design, we fabricated optical fibre which made it possible in our experiments to stretch pulses with a centre wavelength of 1030 nm and a width of 10 nm to 440 ps and then compress them by a grating compressor to 370 fs.

2. Theory

To compress amplified pulses, CPAs typically use grating-pair compressors. The use of grating compressors is economically attractive. In the case of a pulse duration above several hundred picoseconds, only such compressors can be utilised. In this work, we shall also compress pulses in a grating compressor, so it is most logical to begin solving the problem at hand – to produce stretcher fibre – by analysing the grating compressor design and parameters (β_2 and β_3). With these parameters in mind, we will design stretcher fibre.

The simplest grating-pair compressor design is the so-called Treacy configuration [4] (Fig. 1, bottom left). The highest achievable dispersion (i.e. the delay due to the compressor) is determined by several parameters: centre wavelength (λ) and spectral width ($\Delta\lambda$) of the pulses to be compressed, the ruling density of the gratings (f), the angle of incidence of light on the first grating (α), and the width of the second grating (w). In our calculations, we use characteristics of transmissive diffraction gratings at our disposal, TDG1 and

K.K. Bobkov, A.E. Levchenko, M.E. Likhachev Dianov Fiber Optics Research Center, Prokhorov General Physics Institute, Russian Academy of Sciences, ul. Vavilova 38, 119333 Moscow, Russia; e-mail: wittkoss@gmail.com;
M.Yu. Salganskii G.G. Devyatykh Institute of Chemistry of High-Purity Substances, Russian Academy of Sciences, ul. Tropinina 49, 603950 Nizhny Novgorod, Russia;
D.V. Ganin, D.V. Khudyakov Physics Instrumentation Center, Prokhorov General Physics Institute, Russian Academy of Sciences, Kaluzhskoe sh. 4/1, Troitsk, 108840 Moscow, Russia;
A.D. Lyashedko Optosystems Ltd., Kaluzhskoe sh. 4/1, Troitsk, 108840 Moscow, Russia

Received 22 June 2021
Kvantovaya Elektronika **51** (10) 894–900 (2021)
Translated by O.M. Tsarev

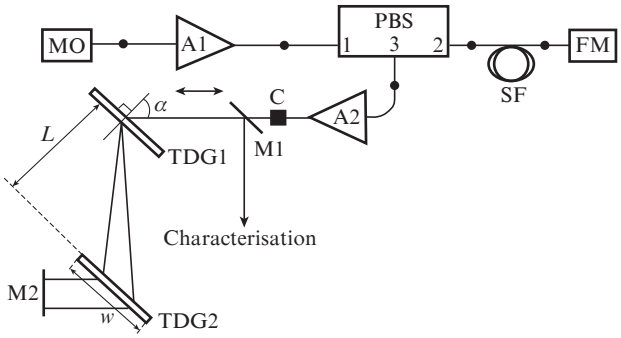

Figure 1. Schematic of the experimental setup: (MO) master oscillator; (A1, A2) fibre amplifiers; (PBS) polarising beam splitter; (SF) stretcher fibre; (FM) Faraday mirror; (C) collimator; (M1, M2) dielectric mirrors; (TDG1, TDG2) transmissive diffraction gratings; w is the grating width, and α is the angle of incidence of light on the input grating.

TDG2, with $f = 1600$ lines per millimetre, intended for operation at $\lambda = 1060$ nm and $\alpha = 58°$ (at this angle, diffraction efficiency exceeds 94%; according to the manufacturer, diffraction efficiency above 90% can be reached in the α range 47°–66°). The width of the second grating is $w = 0.13$ m. The spectral width of the pulses to be compressed is taken to be 10 nm, with a centre wavelength $\lambda = 1065$ nm (these parameters correspond to a transform-limited Gaussian pulse duration under 200 fs).

The maximum time delay due to the compressor under consideration (here and in what follows, light dispersed by TDG1 is assumed to span the entire width of TDG2) can be estimated using geometric optics analysis:

$$\tau = \frac{2w[\sin(\alpha_{-1} + D_\alpha) + \sin\alpha]}{c}, \qquad (1)$$

where α_{-1} is the angle of diffraction into the –1 order; $D_\alpha = -f/\sqrt{1-(\sin\alpha - \lambda f)^2}$ is the angular dispersion of the grating; and c is the speed of light. The maximum permissible separation between parallel gratings for spanning TDG2 can be estimated using the relation

$$L = \frac{w}{\tan(\alpha_{-1} + D_\alpha \Delta\lambda) - \tan\alpha_{-1}}. \qquad (2)$$

It follows from (1) and (2) that the maximum delay is about 1.4 ns at angles of incidence in the range 47°–66°. The delay is a weak function of the centre wavelength of the light being compressed (at wavelengths in the 1 μm range). However, as α decreases to critical values at which the diffraction angle approaches 90°, the delay decreases with increasing wavelength (Fig. 2a, $\alpha = 47°$).

The second- and third-order dispersion coefficients (β_2 and β_3) for the compressor design under discussion can be calculated using the relations [5]

$$\beta_2 = -\frac{\lambda^3 L f^2}{\pi c^2}[1-(\lambda f - \sin\alpha)^2]^{-3/2},$$
$$\beta_3 = -\frac{3\lambda}{2\pi c}\frac{1+\lambda f\sin\alpha - \sin^2\alpha}{1-(\lambda f-\sin\alpha)^2}\beta_2. \qquad (3)$$

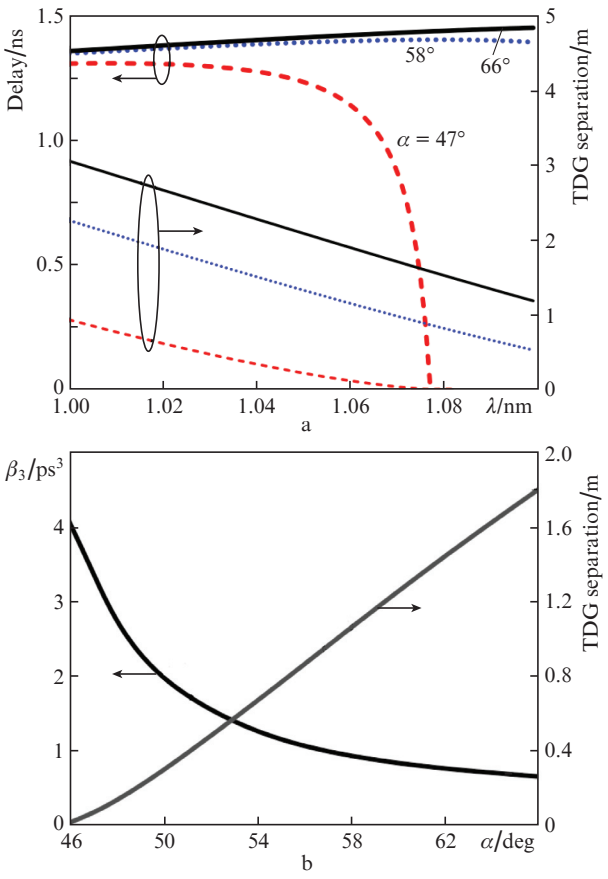

Figure 2. (a) Maximum attainable delay for light with a spectral width of 10 nm and grating separation as functions of wavelength; (b) maximum attainable third-order dispersion β_3 and grating separation for light with a centre wavelength of 1065 nm and spectral width of 10 nm as functions of the angle of incidence of light, α, on the first diffraction grating.

According to (3), as the angle of incidence of light on the input grating of the compressor decreases, the maximum attainable second-order dispersion varies relatively little (at a centre wavelength of 1065 nm and α in the range 47°–66°, β_2 changes from –63 to –86 ps^2, respectively), but the necessary grating separation (at a constant spectral width of pulses $\Delta\lambda = 10$ nm) then changes by more than one order of magnitude (Fig. 2a). At the same time, a negative consequence of a decrease in angle is a rise in third-order dispersion (Fig. 2b), which should be compensated.

Thus, operation at small angles of incidence (α) allows one to make a rather compact compressor, but the second-order dispersion of the stretcher fibre should vary very rapidly with wavelength. It is then possible to find an angle of incidence at which a compact compressor can be made at any wavelength.

Consider now stretcher fibre. In fibre optics, it is convenient to use not second-order dispersion but the dispersion parameter D, which is related to β_2 by $D = -(2\pi c/\lambda^2)\beta_2$ and allows one to easily estimate the approximate pulse duration after propagation through fibre as $\tau \approx Dl\Delta\lambda$, where l is the fibre length. Using the above relation for D and taking into account that $\beta_3 = \partial\beta_2/\partial\omega$ (where ω is frequency), we can derive a relation between D in the fibre and the β_3/β_2 ratio of the compressor:

$$\frac{\beta_3}{\beta_2} = -\left(2 + \frac{D'}{D}\lambda\right)\frac{\lambda}{2\pi c}, \quad (4)$$

where $D' = \partial D/\partial\lambda$ is the slope of the dispersion parameter. It is convenient to use the D'/D ratio for characterisation of fibre because this quantity is independent of the fibre length (hereafter, we assume that the fibre length is always adjusted so as to compensate for the second-order dispersion at an operating wavelength of 1065 nm).

Using (3) and (4), we obtain the dependences of D'/D required for fibre–compressor matching (Fig. 3). It is seen from Fig. 3 that, at $\lambda = 1065$ nm, the required value of D'/D can be tuned over a wide range by varying the angle of incidence of light on the diffraction grating: from 11 μm^{-1} at $\alpha = 66°$ to 87 μm^{-1} at $\alpha = 47°$.

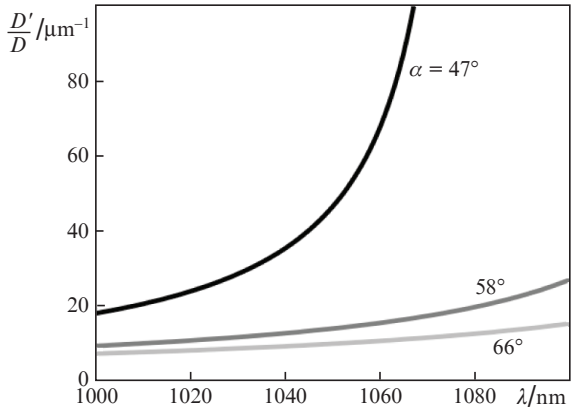

Figure 3. $D'/D(\lambda)$ curves necessary for matching stretcher fibre to a grating compressor at different angles of incidence α.

As pointed out above, the third-order dispersion in standard fibres for operation in the 1 μm range (e.g. in PM980 fibre, which is used in the fabrication of commercially available multiplexers, isolators, circulators, etc.) has the same sign ($\beta_3 > 0$) as the third-order dispersion in a grating compressor, i.e. the dispersion parameter in this region is negative but has a positive slope D'. In optical fibre, light propagates in transverse modes, whose dispersion characteristics depend on the dispersion of the fibre material and the guidance properties of the fibre. Since we cannot influence the dispersion of silica glass, characteristics of the dispersion parameter curve of a transverse mode of fibre are, roughly speaking, dependent on how its electric field distribution varies with the wavelength of light propagating in this mode. In practice, this means that a negative slope of the dispersion parameter can be ensured by producing near-cutoff propagation conditions for the operating mode. In the case of step-index fibres, including PM980, all modes except the fundamental one have cutoff. However, if the fibre core is surrounded by a depressed layer – a circular layer whose refractive index is smaller than that of undoped silica glass (so-called W profile fibre) – the fundamental mode also has a cutoff wavelength [6].

Previously, our group proposed a fibre design with such an index profile for stretching pulses with a centre wavelength of 1030 nm [1]. It had the following parameters: core/cladding diameters, 1.3/125 μm; depressed layer thickness, 3.5 μm; refractive-index difference between core/depressed layer and undoped silica glass dn = 0.04/–0.01. As a result, at λ = 1030 nm the dispersion parameter D was –240 ps nm^{-1} km^{-1} and the D'/D ratio was 7.5 μm^{-1}. The fibre was used to stretch pulses with a centre wavelength of 1030 nm and a width of 16 nm, generated by a femtosecond oscillator, to a duration of ~180 ps. The stretched pulses were amplified and then compressed in a grating-pair compressor (1600 lines per millimetre; angle of incidence, 55.5°; grating separation, 0.12 m) to 270 fs at a transform-limited pulse duration near 100 fs. It should be noted that autocorrelation traces showed that the pulses had a pedestal.

The main problem with the proposed fibre design was the necessity to fabricate a small diameter core. The diffusion of the germania used to raise the refractive index of silica glass causes 'smearing' of the refractive index profile (RIP) in real fibre, leading to a considerable change in the dispersion parameter D and a decrease in the D'/D ratio and fundamental mode cutoff wavelength. Figure 4 illustrates how diffusion influenced the shape of the RIP across the core and how the resultant changes impacted the dispersion parameter curve (Fig. 4, inset). It is seen that diffusion influenced not only the dispersion parameter and the slope of the curve but also the fundamental mode cutoff wavelength (reducing it from 1110 nm in the model fibre to 1085 nm in the real one). It is worth noting that another drawback to a small core size is a low threshold for nonlinear effects (SRS, self-phase modulation), which have a negative effect on pulse compression effectiveness. In addition, the fibre in question was shown to have a large loss (1.5 dB) when fusion-spliced to standard fibre because of the large mode field diameter difference.

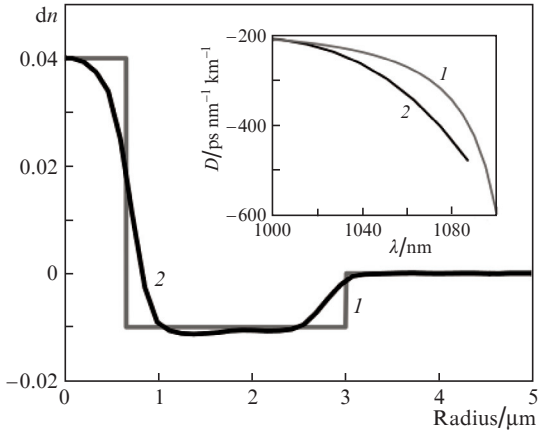

Figure 4. (*1*) Model RIP and (*2*) RIP across the fibre fabricated previously. Inset: calculated dispersion parameter D for the model RIP and measured dispersion parameter of the real fibre (data from Ref. [1]).

Note that yet another problem with the use of double-clad fibre is that the fundamental mode cutoff and operating wavelengths differ little. As a result, even small variations in fibre diameter lead to considerable variations in fundamental mode cutoff wavelength, so there is the risk that a part of a pulse being stretched and compressed will be lost because of the large leakage loss.

Previously, a more complex way of controlling the dispersion slope was proposed: a second ring, with an increased

refractive index, was made around the first ring (a layer with a reduced refractive index around the core) to form a so-called triple-clad fibre. Such a fibre design was first used to tailor the shape of the dispersion parameter curve (see e.g. Ref. [2]). At the same time, to match third- and fourth-order dispersion to a grating compressor, Ramachandran et al. [3] had to use an additional module with fibre supporting higher mode propagation. Even though Grüner-Nielsen et al. [2] did not specify exact parameters of the fibre designed by them (size and refractive index of the core and the layers surrounding it), we suppose that one of the causes of their failure to completely match the dispersion of the triple-clad fibre to a grating compressor was technological limitations that prevented them from minimising the refractive index of the depressed layer. As a rule, the use of standard modified chemical vapour deposition techniques allows one to ensure a refractive index depression at a level of -0.005 [7]. According to our calculations, it is the maximum depression level that limits the maximum attainable second- and third-order dispersion. In particular, maintaining the refractive index difference between the depressed layer and undoped silica glass at a level of -0.005 and varying the refractive index and radius of the core, the width of the depressed layer, and the dimensions and refractive index of the circular layer, while ensuring single-mode operation, we obtained a maximum D'/D ratio at a level of 11 μm^{-1} (at a wavelength of 1065 nm).

It should be noted that, previously, Guryanov et al. [8] proposed a process for growing a highly fluorinated layer by modified chemical vapour deposition (MCVD), which made it possible to reach a refractive index depression down to -0.011, substantially extending the possibilities of designing the index profile of dispersion-compensating fibre.

Since the triple-clad fibre design under consideration has six degrees of freedom (core radius, thicknesses of the first and second circular layers, and the refractive indices of the core and the first and second circular layers), adjusting these parameters requires considerable effort and time. At the same time, two restrictions slightly simplify the problem. (1) The MCVD process used by us is incapable of producing glass with a refractive index lower than that of undoped silica glass by more than 0.011 (i.e. with $dn = -0.011$). (2) The core should support propagation of only the fundamental mode. Taking into account these restrictions, we wrote software using which, and roughly testing the above parameters, we searched for a suitable fibre RIP from the viewpoint of the dispersion parameter and its slope in the wavelength range of interest, with the D'/D ratio at $\lambda = 1065$ nm lying in the above-mentioned range (11–87 μm^{-1}).

Figure 5 shows two RIPs obtained as a result of simulation. We examined two extreme cases: fibre with a relatively low limiting D'/D value (fibre 1) and fibre with D'/D near the limit (fibre 2). The parameters of fibre 1 were as follows: core radius, 1.6 μm; the width of the first and second circular layers, 1.57 and 1.18 μm, respectively; dn of the core, first circular layer, and second circular layer, 0.01, -0.01, and 0.002, respectively. Fibre 2 had the following parameters: core radius, 1.6 μm; the width of the first and second circular layers, 2.74 and 1.27 μm, respectively; dn of the core, first ring, and second ring, 0.01, -0.009, and 0.003. As seen in Fig. 6, the dispersion parameter curves of the model RIPs agree well with those of a compressor in a wide wavelength range, which indicates that the fibres are matched to the compressor not only in third-order dispersion but also in at least fourth-order dispersion. The D'/D ratios calculated for a wavelength of 1065 nm using the obtained curves were 18 and 85 μm^{-1} for the model RIPs of fibres 1 and 2, respectively.

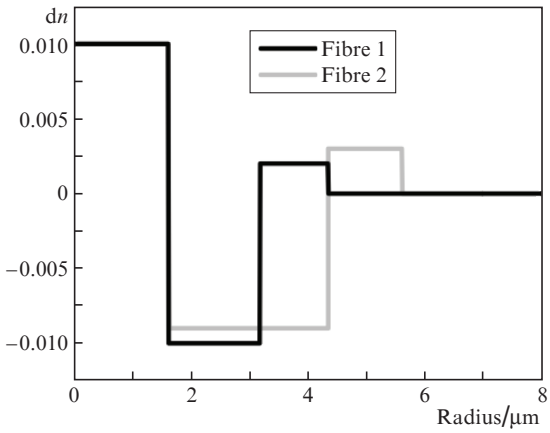

Figure 5. Model RIPs of the triple-clad fibres.

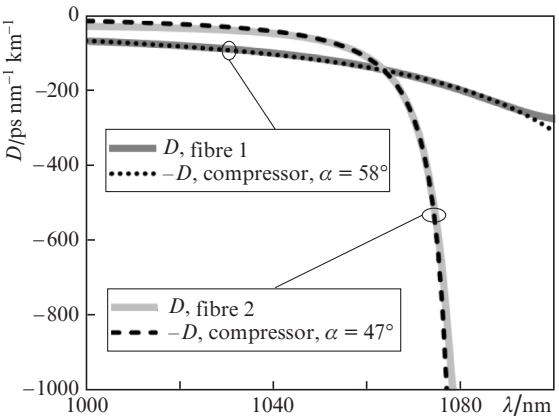

Figure 6. Dispersion parameter (D) curves of the model RIPs and a compressor at different angles of incidence (α).

To evaluate the match between the fibres under consideration and the compressor in terms of the dispersion parameter, we plot the mismatch $\Delta t(\delta\lambda)$, defined as the product of the difference between the dispersion parameters of the compressor (D_c) and fibre (D_f) with detuning $\delta\lambda$: $(D_c - D_f)\delta\lambda$ (the detuning $\delta\lambda$ was measured from the centre wavelength, 1065 nm) (Fig. 7a). D_c was calculated for a compressor adjusted to the optimal angle. The physical meaning of Δt is the estimated duration of the incompressible pedestal at the base of a compressed pulse. As seen from Fig. 7a, at a spectral width $\Delta\lambda = 10$ nm the mismatch for fibre 1 does not exceed 0.5 ps. In previous work [1], the mismatch at a spectral width of 10 nm was 1.5 ps and the compressed pulse duration was about 300 fs. This leads us to assume that, at a mismatch between the extreme points at a level of 1 ps, the compressed pulse duration will be below a few hundred femtoseconds. At the same time, in the case of fibre 2, made for an angle $\alpha =$

47°, the 1-ps width of the matched spectrum is just 4 nm. It is also worth specifying that, in the case of fibre 2, a small deviation (a fraction of a degree) from the optimal angle of incidence of light on the input grating of the compressor leads to a sharp drop in the width of the matched spectrum, whereas in the case of fibre 1 a match width of 10 nm is ensured by a much coarser angle tuning (Fig. 7b).

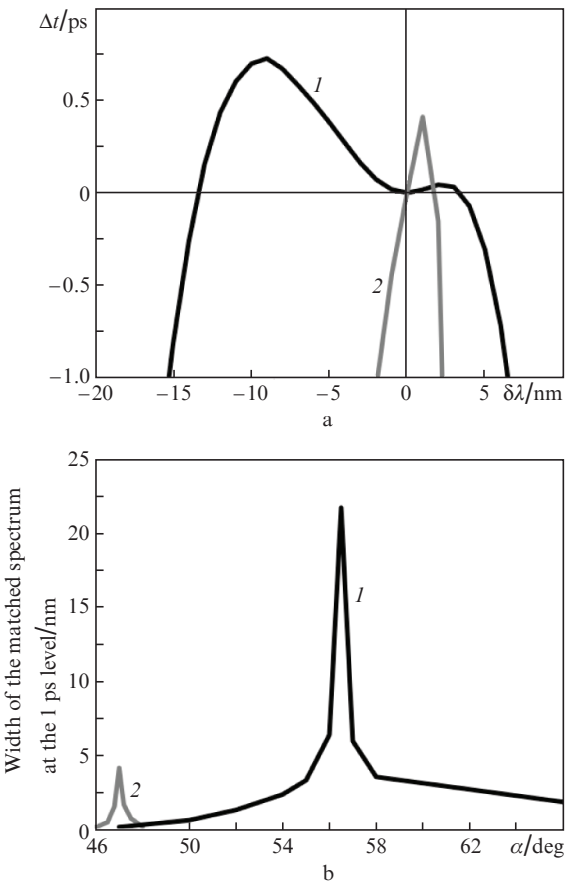

Figure 7. (a) Calculated dispersion parameter mismatch as a function of the detuning δλ from the wavelength 1065 nm and (b) calculated width of the matched spectrum at the 1 ps level as a function of the angle of incidence of light on the first grating of the compressor for fibres (*1*) 1 and (*2*) 2. The calculations were made for a centre wavelength of 1065 nm.

3. Experimental

A fibre preform produced by MCVD had RIP parameters approaching the optimal ones obtained by simulation in the preceding section (Fig. 5, fibre 1). The preform was drawn into fibre, in which the dispersion parameter D was determined using interferometry [9] (-150 ps nm^{-1} km^{-1} at a wavelength of 1030 nm) and the D'/D ratio was calculated (Fig. 8). It is worth noting that the model RIP was reproduced in the preform not quite accurately, so the fundamental mode cutoff wavelength was near the operating wavelength and the fibre was bend-sensitive in this region. In particular, the measured loss in the fibre wound onto a 50-cm-diameter spool was above 800 dB km^{-1} at a wavelength of 1065 nm and 37 dB km^{-1} at a wavelength of 1030 nm. For this reason, in subsequent pulse stretching and compression experiments we had to deal with chirped pulses with a centre wavelength of 1030 nm, rather than 1065 nm. The fibre supported propagation of only the fundamental mode. The loss due to fusion splicing to PM980 standard fibre was 1.1 dB.

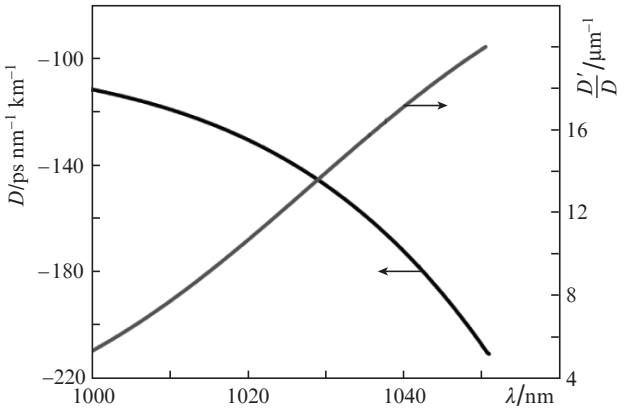

Figure 8. Measured dispersion parameter D and calculated D'/D ratio as functions of wavelength.

A 200-m length of the fibre was used to stretch 6.5-ps pulses with a centre wavelength $\lambda = 1030$ nm, spectral width of 10 nm, and repetition rate of 27.2 MHz, generated by an in-house built master generator of chirped pulses. The stretched pulses were then compressed in a grating compressor (Fig. 1). In all parts of the system, except in the fibre produced by us, use was made of Panda-type polarisation-maintaining fibre, so to maintain the polarisation state of pulses transmitted through the fibre under study we used a fibre polarisation beam splitter and a Faraday mirror with an output fibre pigtail. Owing to the use of the Faraday mirror, the stretcher fibre length was increased essentially twofold, so the induced dispersion also increased. The extinction of the stretched pulses was above 22 dB. At the master oscillator and fibre inputs, light was amplified, and the gain was adjusted so that the spectrum of pulses propagating through the system remained unchanged. The average pulse power (energy) at the outputs of the master oscillator, first amplifier, second amplifier, and compressor was 2.5, 10, 10, and 9 mW (0.092, 0.368, 0.368, and 0.331 nJ), respectively. As shown earlier [10], 10 mW of average power is sufficient for gain saturation in ytterbium-doped tapered fibre, so stretched pulses will subsequently be amplified in tapered fibre. Figure 9 shows spectra of pulses at the outputs of the master oscillator, first amplifier, second amplifier, and compressor. It is seen that the propagation of pulses through the stretcher fibre narrows down their spectrum to 6 nm, which is caused by the large transmission loss in the fibre (in particular, the loss at a wavelength of 1040 nm was 241 dB km^{-1}). The stretched pulse duration is 440 ps (Fig. 10, orange continuous line), which differs from the calculated pulse duration (600 ps according to the relation for τ in Section 2) and can be accounted for by the above-mentioned narrowing of the spectrum of pulses because of the high level of losses.

Stretched pulses were compressed in a compressor comprising two parallel transmissive diffraction gratings (1600 lines per millimetre, optimal angle of incidence of light for

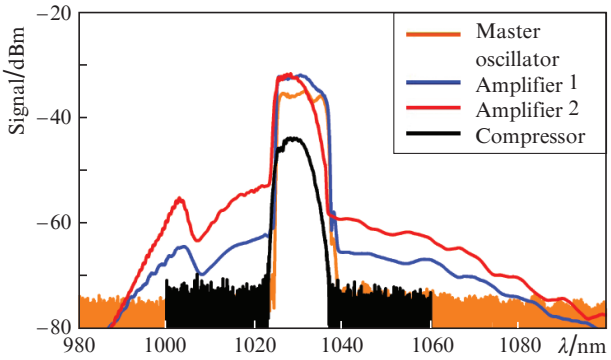

Figure 9. (Colour online) Spectra of pulses at the outputs of the different components of the experimental setup schematised in Fig. 1.

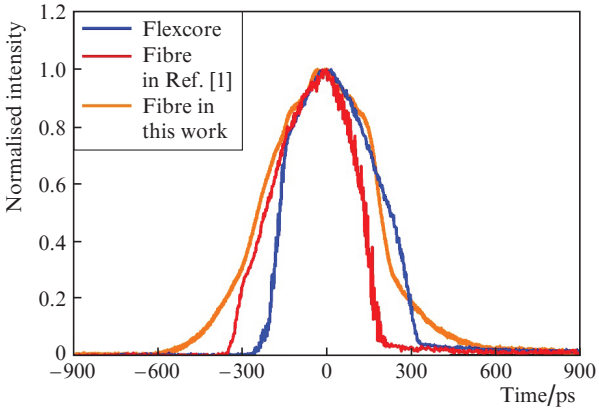

Figure 10. (Colour online) Duration and shape of stretched pulses obtained using different optical fibres.

fibre–compressor matching in terms of third-order dispersion $\alpha = 54°$) separated by 54 cm. The duration of the compressed pulses (under the assumption that they had a Gaussian shape) was 370 fs (Fig. 11, orange line), and the integrated fraction of power in the pedestal was 19%. The autocorrelation trace of a pulse shows a weak peak near a delay time of 5 ps, due to the fact that the beam splitter in the autocorrelator used (Inrad 5-14b) is plane-parallel rather than wedged. For this reason, the observed peak corresponds to autocorrelation of the beam reflected from the backside of the beam splitter. It is worth noting that we were able to compress pulses of the master oscillator to 290 fs (Fig. 11, black line), even though their spectral width was 10 nm, against 6 nm in the case of pulses transmitted through the stretcher fibre under investigation.

For comparison, we carried out an analogous experiment using an about 420-m length of standard telecom fibre Flexcore (dispersion parameter $D = -41$ ps nm^{-1} km^{-1} at $\lambda = 1030$ nm) and fibre from previous work [1], which had only one circular layer and a dispersion parameter $D = -240$ ps nm^{-1} km^{-1} at $\lambda = 1030$ nm and was about 78 m long. In the case of Flexcore fibre, the stretched pulse duration was 390 ps (Fig. 10, blue line). Since it appeared impossible to match this fibre to the compressor, the latter was not readjusted, and the angle of incidence of light remained unchanged (54°). We were able to compress stretched pulses to 570 fs (Fig. 11, blue line) at a grating separation of 38 cm, but the fraction of power in the incompressible pulse pedestal

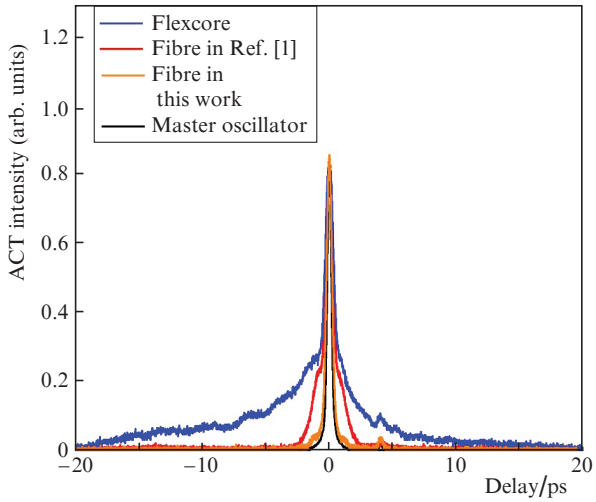

Figure 11. (Colour online) Autocorrelation traces of compressed pulses obtained using different optical fibres and a compressed pulse of the master oscillator.

was 77%. In the case of the fibre from previous work [1], the stretched pulse duration was 360 ps (Fig. 10, red line). For fibre–compressor matching in terms of third-order dispersion, the compressor was readjusted to an angle of incidence of 71° and the grating separation was 80 cm, which allowed stretched pulses to be compressed to 460 fs (Fig. 11, red line), with the fraction of power in the pedestal being 45%. Thus, the best result was obtained with the fibre produced in this work: it is owing to it that we were able to obtain the smallest fraction of power in the pedestal (19% against 45% in the fibre from previous work [1] and 77% in Flexcore standard fibre). The use of the fibre proposed in this study allowed us to obtain the shortest pulse duration (370 fs against 460 fs for the fibre from previous work [1] and 570 fs for Flexcore standard fibre).

4. Conclusions

We have studied the design of a compressor comprising two parallel transmissive diffraction gratings in the Treacy configuration. It has been shown that, by reducing the angle of incidence of pulses on the input diffraction grating, it is possible to produce a very compact pulse compression system (with a grating separation near 20 cm) at a compensable delay near 1.4 ns. Using numerical simulation, we have calculated a triple-clad stretcher fibre design which is excellently matched to the compressor in terms of second- and third-order dispersion in the 1 μm range. One of the calculated designs has made it possible to produce optical fibre with a dispersion parameter $D = -140$ ps nm^{-1} km^{-1} and $D'/D = 14$ μm^{-1} at a wavelength of 1030 nm. The fibre has been used to stretch 6.5-ps pulses with a centre wavelength of 1030 nm and spectral width of 10 nm to 440 ps. The stretched pulses have been compressed in the grating-pair compressor to 370 fs, with the fraction of power in the pedestal being just 19%, which is significantly better than results obtainable using standard fibre (with a step index profile) and even fibre specially designed for resolving such problems [1].

Acknowledgements. This work was supported by the Russian Science Foundation (Grant No. 20-79-00283).

References

1. Khudyakov D.V., Ganin D.V., Lyashedko A.D., Likhachev M.E., Senatorov A.K., Salgansky M.Y., Vartapetov S.K. *J. Opt. Soc. Am. B*, **36**, 3066 (2019).
2. Grüner-Nielsen L., Jakobsen D., Jespersen K.G., Pálsdóttir B. *Opt. Express*, **18**, 3768 (2010).
3. Ramachandran S., Ghalmi S., Nicholson J.W., Yan M.F., Wisk P., Monberg E., Dimarcello F.V. *Opt. Lett*., **18**, 2532 (2006).
4. Treacy E.B. *IEEE J. Quantum Electron*., **5**, 454 (1969).
5. Kane S., Squier J. *IEEE J. Quantum Electron*., **31**, 2052 (1995).
6. Kawakami S., Nishida S. *IEEE J. Quantum Electron*., **10**, 879 (1974).
7. Andreev A.G., Dukel'skii K.V., Ermakov V.S., Eron'yan M.A., Kryukov I.I., Petrovskii G.T., Serkov M.M., Tsibinogina M.K. *Glass Phys. Chem*., **32**, 33 (2006).
8. Guryanov A.N., Salganskii M.Y., Khopin V.F., Kosolapov A.F., Semenov S.L. *Inorg. Mater*., **45**, 823 (2009).
9. Tateda M., Shibata N., Seikai S. *IEEE J. Quantum Electron*., **17**, 404 (1981).
10. Bobkov K., Andrianov A., Koptev M., Muravyev S., Levchenko A., Velmiskin V., Aleshkina S., Semjonov S., Lipatov D., Guryanov A., Kim A., Likhachev M. *Opt. Express*, **25**, 26958 (2017).